DOI:10.1021/jf904089q

JOURNAL OF AGRICULTURAL AND FOOD CHEMISTRY
ARTICLE

Properties of Synthetic Homoisoflavonoids To Reduce Oxidants and To Protect Linoleic Acid and DNA against Oxidation

YAN-FENG LI, ZAI-QUN LIU,* AND XU-YANG LUO

Department of Organic Chemistry, College of Chemistry, Jilin University, Changchun 130021, China

3-(2′-, 3′-, and 4′-Hydroxybenzylidene)-7-methoxychroman-4-one (*o*-, *m*-, and *p*-HBMC) was synthesized for the clarification of the influence of the hydroxyl group at the B ring on the antioxidant activity of homoisoflavonoid. The three homoisoflavonoids used herein can reduce peroxynitrite. *p*-HBMC exhibited high activity to reduce singlet oxygen. Furthermore, *o*-, *m*-, and *p*-HBMC can scavenge the 2,2′-azinobis(3-ethylbenzothiazoline-6-sulfonate) cationic radical ($ABTS^{\bullet+}$) and 2,2′-diphenyl-1-picrylhydrazyl (DPPH) and galvinoxyl radicals. The rates of *o*-HBMC trapping of DPPH and galvinoxyl radicals were higher than those of *m*- and *p*-HBMC, whereas *m*-HBMC can trap $ABTS^{\bullet+}$ rapidly. *o*-HBMC was found to possess high activity in the β-carotene−linoleic acid bleaching test and to protect methyl linoleate against 2,2′-azobis(2-amidinopropane hydrochloride) (AAPH)-induced oxidation efficiently. Finally, *o*-HBMC served as a prooxidant in Cu^{2+}/glutathione (GSH)- and hydroxyl radical-mediated oxidations of DNA. *m*- and *p*-HBMC protected DNA against hydroxyl radical-mediated oxidation of DNA effectively, and *o*- and *p*-HBMC behaved as antioxidants to protect DNA against AAPH-induced oxidation. Thus, the hydroxyl group attaching to the ortho- and para-positions in the B ring was of importance for the homoisoflavonoid's enhancement of antioxidant activity.

KEYWORDS: Homoisoflavonoid; oxidative stress; antioxidant; prooxidant; oxidation of DNA; oxidation of polyunsaturated fatty acid

INTRODUCTION

Flavonoids are widely spread in diets and medicinal herbs (*1*). These compounds are grouped in distinct subclasses including the flavonols, flavones, isoflavonoids, flavanons, flavanols, proanthocyanidins, and anthocyanidins (*2*). Flavonoids as antioxidants are usually employed in the medicinal, agricultural, and food industries (*3*). Despite the natural resource of flavonoids (*4*), many methods have also been developed to synthesize flavonoids (*5*) to change their bioactivities (*6*). Homoisoflavonoids (3-benzylidene-4-chromanones) are isomers of flavonoids and exhibit different biological activities because of hydroxyl groups attaching to different positions (*7*). Homoisoflavonoids were researched by density functional theoretic (DFT) calculation and by electron paramagnetic resonance (EPR) spectra. It was found that hydroxyl groups at the B ring in homoisoflavonoids play the main role in scavenging radicals (*8*). Meanwhile, a large amount of research work on the natural homoisoflavonoids also reveals that the bioactivities of homoisoflavonoids are mainly ascribed to the amount and position of the hydroxyl group at the B ring (*9*, *10*). Because the natural homoisoflavonoids usually contain many hydroxyl groups at various positions (*11*), it is difficult to identify the impact of a single hydroxyl group at a certain position on the antioxidant effectiveness of homoisoflavonoids. Thus, the relationship between the structure of a homoisoflavonoid and its antioxidant activity should be clarified by using synthetic homoisoflavonoids with a single hydroxyl group attaching to the *o*-, *m*-, or *p*- position in the B ring. Synthesis of homoisoflavonoids is based usually on the condensation of 4-chromanones with aromatic aldehydes in the presence of acidic or basic catalyst (*7*). In the present work, *o*-, *m*-, and *p*-hydroxybenzaldehydes were used for the synthesis of 3-(2′-hydroxybenzylidene)-7-methoxychroman-4-one (*o*-HBMC), 3-(3′-hydroxybenzylidene)-7-methoxychroman-4-one (*m*-HBMC), and 3-(4′-hydroxybenzylidene)-7-methoxychroman-4-one (*p*-HBMC), respectively (see eq **1**).

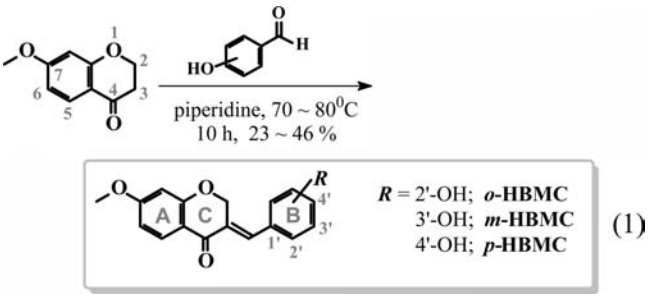

(1)

The aim of the present work is to investigate the influence of the hydroxyl position on the antioxidant effectiveness of the homoisoflavonoid. For that, the antioxidant capacities of *o*-, *m*-, and *p*-HBMC are compared in chemical and biological experimental

*Address correspondence to this author at the Department of Organic Chemistry, College of Chemistry, Jilin University, No. 2519 Jiefang Rd., Changchun 130021, China (e-mail zaiqun-liu@jlu.edu.cn).

 Published on Web 03/03/2010

systems. Chemical experimental systems are composed of reducing peroxynitrite ($ONOO^-$) and singlet oxygen ($^1O_2$), scavenging 2,2′-azinobis(3-ethylbenzothiazoline-6-sulfonate) cationic radical ($ABTS^{\bullet+}$), 2,2′-diphenyl-1-picrylhydrazyl (DPPH) and galvinoxyl radicals, bleaching β-carotene in linoleic acid (LH)−Triton X-100 emulsion, and protecting methyl linoleate against 2,2′-azobis(2-amidinopropane hydrochloride) (AAPH, R—N═N—R, R = $-CMe_2C(=NH)NH_2$)-induced oxidation. Biological experimental systems include the protection of DNA against the oxidation induced by AAPH, Cu^{2+}/glutathione (GSH), and hydroxyl radical ($^{\bullet}OH$), respectively. Positive control compounds such as Trolox or quercentin were not used because the antioxidant effectiveness of Trolox or quercentin screened in these experimental systems has been already reported elsewhere.

MATERIALS AND METHODS

Materials and Instrumentation. The diammonium salt of 2,2′-azinobis(3-ethylbenzothiazoline-6-sulfonate) (ABTS) and DPPH and galvinoxyl radicals were purchased from Fluka Chemie GmbH, Buchs, Switzerland. AAPH, the naked DNA sodium salt, methyl linoleate, linoleic acid, and 4-nitroso-*N*,*N*-dimethylaniline (NDMA) were purchased from Acros Organics, Geel, Belgium. Other agents were of analytical grade and used directly. *o*-, *m*-, and *p*-HBMC were synthesized following the methodology described by Siddaiah et al. (*7*) (see the Supporting Information). The structures were identified by ^1H and ^{13}C NMR (Varian Mercury 300 NMR spectrometer), and the purities of *o*-, *m*-, and *p*-HBMC were identified by high-performance liquid chromatography and were >98%.

Reducing Peroxynitrite Assay. $ONOO^-$ (ε_{302} = 1670 M^{-1} cm^{-1}) was prepared following the methodology described by Uppu et al. (*12*), with some modifications. Briefly, a solution of 2.2 mL of 30% H_2O_2 was diluted to 50 mL with water and cooled in an ice/water mixture. Then, 4 mL of 5 M NaOH and 5 mL of 0.04 M diethylenetriaminepentaacetic acid (DTPA, dissolved in 0.05 M NaOH) were added and diluted to 100 mL with water; then, 2.7 mL of isoamyl nitrite was added and vigorously stirred for 5 h at room temperature. The aqueous phase was washed with 6 × 200 mL of dichloromethane, and the surplus H_2O_2 was decomposed by MnO_2 to obtain $ONOO^-$ aqueous solution. To assess the reduction capacity of the homoisoflavonoids, the *o*-, *m*-, and *p*-HBMC and $ONOO^-$ were mixed in 0.1 M NaOH to 20.0 μM and 0.55 mM as the final concentration, respectively. The absorbance of the mixture was scanned from 250 to 550 nm every 15 min.

Quenching Singlet Oxygen. $^1O_2$ was prepared following the methodology described by Moldonado et al. (*13*). Briefly, 10 mM histidine, 10 mM sodium hypochlorite, 10 mM H_2O_2, and 50 μM 4-nitroso-*N*,*N*-dimethylaniline (NDMA) were dissolved in 45 mM sodium phosphate buffer (pH 7.1) to generate $^1O_2$. The scavenging abilities of *o*-, *m*-, and *p*-HBMC were tested by adding various concentrations of the homoisoflavonoids to the aforementioned mixture to a final volume of 2.0 mL. The mixture was incubated at 30 °C for 40 min, and then the absorbance was measured at 440 nm. The percentage of $^1O_2$ quenched by *o*-, *m*-, and *p*-HBMC was calculated as $(A_{detect} - A_{ref})/(A_0 - A_{ref}) \times 100$, where A_0 and A_{ref} were the absorbance before and after the incubation in the control experiment, respectively, whereas A_{detect} was the absorbance after the incubation in the presence of *o*-, *m*-, and *p*-HBMC.

Scavenging $ABTS^{\bullet+}$, DPPH, and Galvinoxyl Radicals. The $ABTS^{\bullet+}$ radical was derived from the oxidation of ABTS salt. Two milliliters of 4.0 mM ABTS aqueous solution was oxidized by 1.41 mM $K_2S_2O_8$ for 16 h, and then 100 mL of ethanol was added to make the absorbance of $ABTS^{\bullet+}$ around 0.70 at 734 nm [$\varepsilon_{ABTS^{\bullet+}}$ = 1.6 × 10^4 M^{-1} cm^{-1} (*14*)]. DPPH and galvinoxyl were dissolved in ethanol to make the absorbance around 1.00 at 517 nm [ε_{DPPH} = 4.09 × 10^3 M^{-1} cm^{-1} (*15*)] and at 428 nm [$\varepsilon_{galvinoxyl}$ = 1.4 × 10^5 M^{-1} cm^{-1} (*16*)], respectively. *o*-, *m*-, and *p*-HBMC were mixed with $ABTS^{\bullet+}$, DPPH, and galvinoxyl radical solutions, respectively, to test the abilities of homoisoflavonoids to scavenge radicals (*17*). The ethanol solution of *o*-, *m*-, or *p*-HBMC was added to the aforementioned radical solutions at room temperature. The final concentrations of *o*-, *m*-, or *p*-HBMC were 1.0 mM to trap $ABTS^{\bullet+}$ solution and 2.0 mM to trap DPPH and galvinoxyl solutions. The absorbance of the radical solutions was recorded, and the decay rate for the radical was calculated on the basis of the corresponding ε.

β-Carotene Bleaching Test and Protection of Methyl Linoleate against AAPH-Induced Oxidation. An emulsion was prepared by dissolving 5.0 mg of β-carotene, 40 mg of linoleic acid (LH), and 400 mg of Triton X-100 in 5.0 mL of $CHCl_3$. After $CHCl_3$ was evaporated under vacuum pressure, 100 mL of oxygen-saturated water was added, and the mixture was shaken under ultrasonic vibration to form a homogeneous β-carotene−LH emulsion (λ_{max} = 460 nm) (*18*). The ethanol solutions of *o*-, *m*-, and *p*-HBMC (0.1 mL) were mixed with 1.9 mL of β-carotene−LH emulsion to make the final concentration of *o*-, *m*-, and *p*-HBMC at 400 μM. The absorbance of the mixture was detected every 1 h and plotted versus time.

The protective effects of *o*-, *m*-, and *p*-HBMC on AAPH-induced oxidation of methyl linoleate were investigated by detecting the decay of the concentration of methyl linoleate (*19*). Methyl linoleate, methyl palmitate (as the internal standard), AAPH, and *o*-, *m*-, or *p*-HBMC were dissolved in *tert*-butanol/H_2O (1:1, v/v) in a test tube with a final concentration at 14.3 mM, 9.3 mM, 40 mM, or 500 μM, respectively. The test tube was incubated at 37 °C to initiate the oxidation. Aliquots were taken out every 100 min, and the concentration of methyl linoleate was analyzed by GC (Hewlett-Packard 1890 equipped with an SE-54 30 m × 0.25 mm capillary column, 0.25 μm film thickness, N_2). The temperatures of the chromatograph chamber, injector, and hydrogen flame ionization detector were 260, 280, and 300 °C, respectively (*19*).

Effects of *o*-, *m*-, and *p*-HBMC on the Oxidation of DNA Mediated by Cu^{2+}/GSH. The oxidation of DNA mediated by Cu^{2+} and GSH was carried out following the methodology described by Reed et al. (*20*), with some modifications. Briefly, DNA, $CuSO_4$, and GSH were dissolved in phosphate-buffered solution (PBS_1: 6.1 mM Na_2HPO_4, 3.9 mM NaH_2PO_4) with the final concentration at 2.0 mg/mL, 5.0 mM, and 3.0 mM, respectively. Dimethyl sulfoxide (DMSO) solutions of *o*-, *m*-, and *p*-HBMC were added with a final concentration at 0.6 mM. The mixture was delivered into test tubes with each containing 2.0 mL. The test tubes were incubated at 37 °C to initiate the oxidation of DNA. Three tubes were taken out every 30 min and cooled immediately, to which 1.0 mL of PBS_1 solution of EDTA (30.0 mM as the final concentration) was added to chelate Cu^{2+}. The tubes were heated in a boiling water bath for 30 min after 1.0 mL of TBA solution (1.00 g of TBA and 0.40 g of NaOH dissolved in 100 mL of PBS_1) and 1.0 mL of 3.0% trichloroacetic acid aqueous solution were added. After the test tubes had cooled to room temperature, 1.5 mL of *n*-butanol was added and shaken vigorously to extract TBA reactive substance (TBARS). The absorbance of the *n*-butanol layer was measured at 535 nm.

Effects of *o*-, *m*-, and *p*-HBMC on $^{\bullet}OH$-Induced Oxidation of DNA. $^{\bullet}OH$ was generated from the reaction between tetrachlorohydroquinone (TCHQ) and H_2O_2 (*21*). DNA and H_2O_2 were dissolved in phosphate-buffered solution (PBS_2: 8.1 mM Na_2HPO_4, 1.9 mM NaH_2PO_4, 10.0 μM EDTA) to a final concentration of 2.0 mg/mL and 2.0 mM, respectively, to which TCHQ and *o*-, *m*-, and *p*-HBMC (dissolved in DMSO as the stock solutions) were added with a final concentration at 4.0 mM and 0.6 mM, respectively. Then, the above mixture was delivered into test tubes with each containing 2.0 mL. The test tubes were incubated at 37 °C for 30 min and cooled immediately. The following operation was the same as for Cu^{2+}/GSH-mediated oxidation of DNA. The absorbances of TBARS in the control experiment and in the presence of HBMC were assigned as A_0 and A_{detect}. The protective effects of *o*-, *m*-, and *p*-HBMC on $^{\bullet}OH$-induced oxidation of DNA were expressed by $A_{detect}/A_0 \times 100$.

Effects of *o*-, *m*-, and *p*-HBMC on AAPH-Induced Oxidation of DNA. AAPH-induced oxidation of DNA was carried out following our previous method (*22*). Briefly, DNA and AAPH were dissolved in PBS_2 with a final concentration at 2.0 mg/mL and 40 mM, respectively. Various concentrations of *o*-, *m*-, and *p*-HBMC (dissolved in DMSO as the stock solution) were added. The following operation was the same as for Cu^{2+}/GSH-mediated oxidation of DNA except that the heating period was 15 min after TBA and trichloroacetic acid were added.

Statistical Analysis. All of the data were the average value from at least three independent measurements with the experimental error within 10%. The equations and the data in figures were analyzed statistically via one-way ANOVA−Dunnett by using Origin 6.0 professional software, and $p < 0.001$ indicated a significant difference.

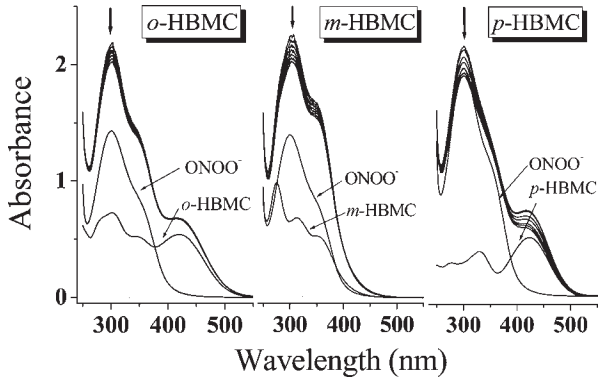

Figure 1. UV−visible spectra of the mixture of 20.0 μM *o*-, *m*-, and *p*-HBMC and 0.55 mM $ONOO^-$. The absorbance at 302 nm was observed to decrease as the mixture was scanned from 250 to 550 nm every 15 min.

RESULTS AND DISCUSSION

Reducing $ONOO^-$ and Quenching $^1O_2$. Some serious diseases have been proved to correlate with the in vivo oxidations mediated by $ONOO^-$ and $^1O_2$ (*23*, *24*). $ONOO^-$ generated from the reaction between isoamyl nitrite and H_2O_2 and $^1O_2$ generated from the mixture of NaClO and H_2O_2 are usually applied to test the reductive ability of antioxidants (*12*, *13*). **Figure 1** is the UV−visible spectra (detected every 15 min) of the mixture of 0.55 mM $ONOO^-$ and 20.0 μM *o*-, *m*-, or *p*-HBMC. The λ_{max} of $ONOO^-$ is 302 nm, whereas the λ_{max} values of *o*-, *m*-, and *p*-HBMC are 300, 275, and 424 nm, respectively. The decrease of absorbance at 302 nm indicates a decrease of the concentrations of $ONOO^-$; that is, $ONOO^-$ is exhausted in the presence of *o*-, *m*-, and *p*-HBMC as the incubation period increases. Thus, *o*-, *m*-, and *p*-HBMC are able to reduce $ONOO^-$.

$^1O_2$ can be detected by measuring the absorbance of NDMA at 440 nm (A_{440}). For example, the decrease of A_{440} from 1.100 to 0.591 indicates that $^1O_2$ oxidizes NDMA to form a colorless product. In the presence of 400 μM *p*-HBMC, the absorbance decreases to just 0.764, indicating that *p*-HBMC instead of NDMA is oxidized by $^1O_2$ and that *p*-HBMC quenches $^1O_2$ actually. The percentage of $^1O_2$ quenched by *p*-HBMC can be calculated as $(0.764 - 0.591)/(1.100 - 0.591) \times 100 = 34.0$. **Figure 2** outlines the relationships between the concentrations of *o*-, *m*-, and *p*-HBMC and the percentages of $^1O_2$ quenched. As observed, more $^1O_2$ molecules are quenched as the concentrations of *m*- and *p*-HBMC increase. Especially, the percentage of $^1O_2$ quenched by *p*-HBMC increases much more rapidly as the concentration of *p*-HBMC increases. *o*-HBMC quenches $^1O_2$ concentration-dependently. The middle concentration of *o*-HBMC has the best activity to quench $^1O_2$, whereas it decreases rapidly when the concentration of *o*-HBMC exceeds 200 μM.

Trapping $ABTS^{\bullet+}$, DPPH, and Galvinoxyl Radicals. Another method to characterize the antioxidant ability is to directly scavenge radicals including $ABTS^{\bullet+}$, DPPH, and galvinoxyl radicals. $ABTS^{\bullet+}$ is always employed to test the total antioxidant capacity because it can react with all phenolic hydroxyl groups (*25*). The interactions of an antioxidant with DPPH and galvinoxyl radicals elicit the ability of the antioxidant to contribute its hydrogen atom to N- and O-centered radicals (*26*, *27*). The absorbances are recorded after *o*-, *m*-, and *p*-HBMC are mixed with $ABTS^{\bullet+}$, DPPH, and galvinoxyl radical solutions. The rates of *o*-, *m*-, and *p*-HBMC to trap $ABTS^{\bullet+}$, DPPH, and galvinoxyl radicals, which were estimated by the product of the slope in the decay of the absorbance and the corresponding ε of the radical, are listed in **Table 1**.

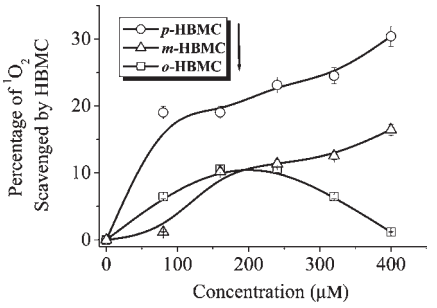

Figure 2. Percentages of $^1O_2$ quenched by various concentrations of *o*-, *m*-, and *p*-HBMC at 30 °C for 40 min.

Table 1. Rates of *o*-, *m*-, and *p*-HBMC To React with Free Radicals

	d[radical]/d*t* (nM min^{-1})		
free radical	*o*-HBMC	*m*-HBMC	*p*-HBMC
$ABTS^{\bullet+}$	1530	1850	1430
DPPH	1320	470	450
galvinoxyl	220	100	60

The rates of *o*-, *m*-, and *p*-HBMC to react with $ABTS^{\bullet+}$ are much faster than those to react with DPPH and galvinoxyl radicals, indicating that the hydroxyl group at the B ring is more active in reducing $ABTS^{\bullet+}$ than in trapping DPPH and galvinoxyl radicals. Especially, *m*-OH has a higher reductive ability to reduce $ABTS^{\bullet+}$. The rates of *o*-, *m*-, and *p*-HBMC to trap DPPH are faster than those to trap galvinoxyl radicals, indicating that the abilities of *o*-, *m*-, and *p*-HBMC to donate their hydrogen atom in OH to a N-centered radical are much higher than their abilities to donate to an O-centered radical. Moreover, *o*-HBMC has the highest rate to trap DPPH and galvinoxyl radicals, demonstrating that the hydrogen atom in *o*-OH can be abstracted by radicals more readily than at other positions. Thus, *o*-OH in homoisoflavonoid plays a causative role in trapping radicals, and *m*-OH is mainly responsible for reducing radicals.

Bleaching β-Carotene in LH Emulsion and Protecting Methyl Linoleate against AAPH-Induced Oxidation. The abundant components of polyunsaturated fatty acids (PUFAs) make lipids and membranes susceptible to oxidation by in vivo reactive oxygen species (ROS), leading to physiological degradations of lipids and membranes and fatal diseases eventually (*28*). LH and its methyl ester are usually employed to be substrates to mimic PUFA undergoing the in vitro oxidative stress. Thus, the antioxidant abilities of *o*-, *m*-, and *p*-HBMC to inhibit autoxidation and radical-induced oxidation of LH are explored as shown in **Figure 3**.

LH and β-carotene can form a homogeneous emulsion in water with Triton X-100 or Tween being surfactant (*18*). As shown in panel **A** of **Figure 3**, the continual decay of the absorbance at 460 nm reveals that β-carotene is depleted successively by peroxyl radical ($LOO^{\bullet}$) generated from the autoxidation of LH. However, the additions of 400 μM *o*-, *m*-, and *p*-HBMC retard the consumption of β-carotene, indicating that *o*-, *m*-, and *p*-HBMC are able to protect LH against the autoxidation. In particular, the decay of the absorbance in the presence of *o*-HBMC is higher than in other lines, indicating that *o*-OH makes homoisoflavonoid an efficient antioxidant to inhibit the autoxidation of LH. The rapid decay of the absorbance in the presence of *m*-HBMC reveals that the antioxidant activity of *m*-OH is lower than that of *o*- and *p*-OH under this experimental condition.

AAPH is a water-soluble peroxyl radical ($ROO^{\bullet}$) resource. Methyl linoleate is used as substrate because the methyl ester of LH is easily evaporated in GC (*19*). As shown in the blank

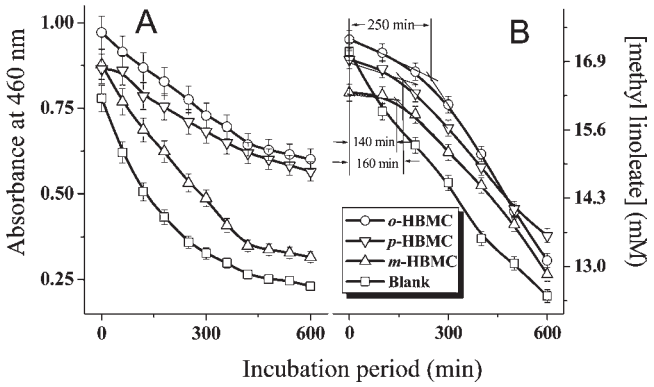

Figure 3. (**A**) Decay of the absorbance at 460 nm of β-carotene−LH emulsion in the presence of 400 μM *o*-, *m*-, and *p*-HBMC. (**B**) Decay of the concentration of methyl linoleate (14.3 mM) in the presence of 40.0 mM AAPH and 500 μM *o*-, *m*-, and *p*-HBMC.

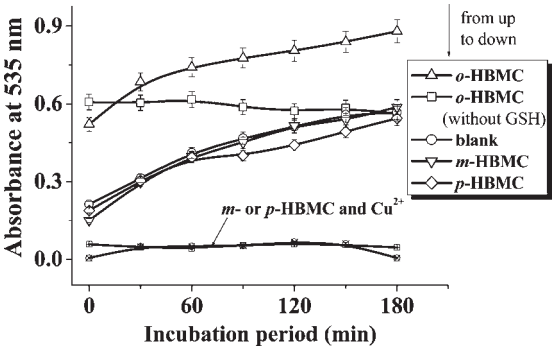

Figure 4. Variety of the absorbance of TBARS in the oxidation of DNA (2.0 mg/mL) mediated by 5.0 mM Cu^{2+} and 3.0 mM GSH in the presence of 0.6 mM *o*-, *m*-, and *p*-HBMC, respectively.

experiment of panel **B** of **Figure 3**, the decay of the concentration indicates that methyl linoleate is depleted in AAPH-induced oxidation as the incubation period increases. The addition of 500 μM *o*-HBMC retards the decrease of the concentration of methyl linoleate for 250 min, indicating that *o*-HBMC can hinder the oxidation of methyl linoleate in this period. The same concentration of *p*-HBMC generates an inhibition period of 160 min, whereas *m*-HBMC results in an inhibition period of 140 min. This result is in agreement with that from the β-carotene bleaching test. Therefore, *o*-OH at the B ring is of importance to the antioxidant effect of homoisoflavonoid on the autoxidation and AAPH-induced oxidation of PUFA.

Protecting DNA against Cu^{2+}/GSH-Induced Oxidation. The destruction of DNA caused by the intracellular GSH and Cu(II) is regarded as carcinogenesis because the GSH radical ($GS^{\bullet}$) is generated in the mixture of Cu(II) and GSH degrades DNA to form propenals. The propenal-related carbonyl compounds can be measured spectrometrically after reacting with TBA (*29*). Thus, carbonyl compounds formed in the case of the oxidation of DNA are also called TBARS.

Figure 4 shows that the absorbance of TBARS increases successively in the blank experiment, indicating that more carbonyl compounds are generated as the incubation period increases. TBARS cannot be formed when Cu(II) or GSH is individually used to interact with DNA (data not shown), demonstrating that Cu(II) or GSH alone cannot drive DNA to form TBARS. More TBARS are generated from the decomposition of DNA mediated by 5.0 mM Cu^{2+} and 3.0 mM GSH as the incubation period increases. The variation of the absorbance in the presence of

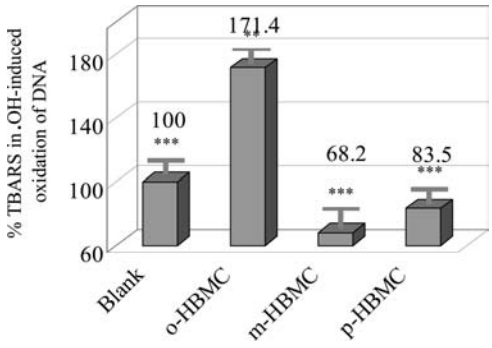

Figure 5. Percentages of TBARS generated from the mixture of 2.0 mg/mL DNA, 2.0 mM H_2O_2, 4.0 mM TCHQ, and 0.6 mM *o*-, *m*-, and *p*-HBMC at 37 °C for 30 min.

m-HBMC (0.6 mM) is almost the same as that in the blank experiment, indicating that *m*-HBMC cannot protect DNA against Cu^{2+}/GSH-mediated oxidation. The variation of the absorbance in the presence of *p*-HBMC approaches that in the blank experiment, revealing that the ability of *p*-HBMC to protect DNA is not obvious. The line of the absorbance in the presence of *o*-HBMC is much higher than that in the blank experiment. The addition of *o*-HBMC accelerates the oxidation of DNA to form TBARS, thus acting as a prooxidant in this case.

Recently, hydroxycinnamic acids were reported to be prooxidant in the mixture of Cu(II) and DNA (*30*). This fact reminds us to clarify whether the redox between Cu^{2+} and homoisoflavonoid also induces the oxidation of DNA. Therefore, Cu^{2+} and *o*-, *m*-, or *p*-HBMC were mixed with DNA to measure TBARS, and the results are outlined in **Figure 4**. The lines of the absorbance generated from Cu^{2+} used in combination with *m*- or *p*-HBMC do not change within the measurement period and are much lower than that in the blank experiment (Cu^{2+} plus GSH). Thus, *m*- and *p*-HBMC used in combination with Cu^{2+} cannot lead to the formation of TBARS. On the other hand, the addition of *o*-HBMC to the mixture of Cu^{2+} and DNA makes the absorbance higher than that in the blank experiment, indicating that *o*-HBMC in the presence of Cu^{2+} behaves as a prooxidant to improve the formation of TBARS. The prooxidant role of *o*-HBMC may be understood in light of the results of Zheng et al. (*30*). In that work, Cu(II) is reduced by the hydroxyl group in hydroxycinnamic acid to form Cu(I). Cu(I) forms a complex with DNA, DNA−Cu(I)OOH, and meanwhile, interacts with O_2 to form O_2^- and H_2O_2. As a result, the interaction between H_2O_2 and DNA−Cu(I)OOH promotes the cleavage of DNA. Thus, in our experiment, *o*-HBMC may reduce Cu(II) to form Cu(I), resulting in the degradation of DNA as shown in eq **2**.

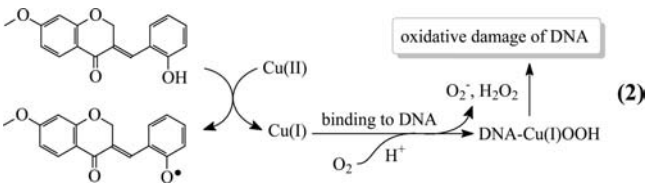

Protecting DNA against $^{\bullet}$OH-Induced Oxidation. $^{\bullet}$OH as an important in vivo ROS resource can be conveniently generated by in vitro Fenton reaction between tetrachlorohydroquinone (TCHQ) and H_2O_2 and be applied to screen the abilities of antioxidants to trap $^{\bullet}$OH (*21*). Malondialdehyde is generated in $^{\bullet}$OH-induced oxidation of DNA and can be detected by forming TBARS. The absorbance of TBARS formed in the presence of homoisoflavonoid is compared with that in the blank experiment. A low percentage of TBARS formed indicates that the corresponding

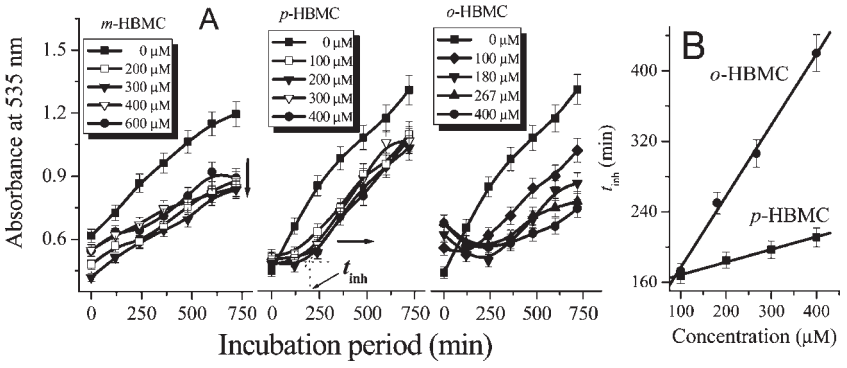

Figure 6. Variety of the absorbance of TBARS in the oxidation of DNA (2.0 mg/mL) induced by 40 mM AAPH and inhibited by various concentration of *o*-, *m*-, and *p*-HBMC (**A**), and the relationships between t_{inh} and the concentrations of *o*- and *p*-HBMC (**B**).

homoisoflavonoid has a strong ability to protect DNA against $^{\bullet}$OH attack. **Figure 5** illustrates the percentages of TBARS formed in $^{\bullet}$OH-induced oxidation of DNA in the presence of 4.0 mM *o*-, *m*-, or *p*-HBMC.

The percentages of TBARS decrease to 68.2 and 83.5% in the presence of *m*- and *p*-HBMC, respectively, indicating that *m*- and *p*-HBMC act as antioxidants to protect DNA, and the activity of *m*-HBMC is higher than that of *p*-HBMC. The percentage of TBARS is as high as 171.4% in the presence of *o*-HBMC, revealing that *o*-HBMC behaves as a prooxidant to destroy DNA, forming much more TBARS.

Protecting DNA against AAPH-Induced Oxidation. The peroxyl radical (ROO$^{\bullet}$) generated from the decomposition of AAPH can abstract a H atom from the C-4′ atom of DNA, causing strand breaks and generating TBARS eventually. Thus, AAPH is usually used to mimic DNA undergoing peroxyl radical-induced oxidative stress. The continual increase of the absorbance in the blank experiment reveals that more TBARS is formed in AAPH-induced oxidation of DNA as the incubation period increases. The additions of various concentrations of *o*-, *m*-, and *p*-HBMC markedly change the absorbance as shown in **Figure 6**.

The additions of various concentrations of *m*-HBMC make the absorbance lower than that in the blank experiment. Meanwhile, the increase of the absorbance slows as the concentration of *m*-HBMC increases. Therefore, the addition of *m*-HBMC retards the amount of TBARS formed in AAPH-induced oxidation of DNA. Moreover, the addition of *p*-HBMC inhibits the increase of the absorbance for a period, implying that *p*-HBMC inhibits the oxidation of DNA to generate an inhibition period (t_{inh}). As shown in **Figure 6**, the t_{inh} can be measured from the cross point of two tangents being related to the inhibition and oxidation periods. The t_{inh} is prolonged as the concentration of *p*-HBMC increases. The relationship between t_{inh} and the concentration of *p*-HBMC is illustrated in panel **B** of **Figure 6**. Thus, *p*-HBMC protects DNA against AAPH-induced oxidation, leading to a concentration-dependent t_{inh}.

The addition of *o*-HBMC to AAPH-induced oxidation of DNA generates a concentration-dependent t_{inh} as well, but the absorbance in the first measurement is higher than that in a blank experiment as the concentration of *o*-HBMC increases. To clarify the reason for this phenomenon, the absorbances of the mixtures of 0.4 mM *o*-HBMC + 2.0 mg/mL DNA and of 0.4 mM *o*-HBMC + 40 mM AAPH were measured. The absorbance is 0.17 in the mixture of *o*-HBMC and DNA, indicating that *o*-HBMC alone cannot oxidize DNA to form TBARS. On the other hand, the absorbance is 0.70 in the mixture of *o*-HBMC and AAPH and decreases to 0.35 when the mixture is incubated at 37 °C for 2 h. This decay of the absorbance is similar to that of 0.4 mM *o*-HBMC employed to protect DNA against AAPH-induced oxidation. Thus, the high absorbance in the first measurement may be ascribed to some colorful products generated from the direct interaction between *o*-HBMC and AAPH, and the antioxidant property of *o*-HBMC may also be derived from *o*-HBMC to trap AAPH directly.

The linear relationship between t_{inh} and the concentration of *p*- and *o*-HBMC can be expressed by eqs **3** and **4**, respectively.

$$t_{inh}\ (\text{min}) = 0.15[p\text{-HBMC}\ (\mu\text{M})] + 153.6 \quad (3)$$

$$t_{inh}\ (\text{min}) = 0.82[o\text{-HBMC}\ (\mu\text{M})] + 93.6 \quad (4)$$

The constants in eqs **3** and **4** are derived from the linear regression analysis to balance the equation, whereas the coefficients reveal the sensitivity of t_{inh} to the variation of the concentration of *p*- and *o*-HBMC. The coefficient in eq **4** (0.82) is ~5.5-fold that in eq **3** (0.15), indicating that t_{inh} depends upon the variation of the concentration of *o*-HBMC more markedly than on the variation of the concentration of *p*-HBMC.

In conclusion, the synthetic homoisoflavonoids with a single hydroxyl group reveal the relationship of homoisoflavonoid structure and antioxidant activity in detail. The hydroxyl group at any position in homoisoflavonoid can reduce $ONOO^-$ and $^1O_2$ and trap radicals. In particular, a hydroxyl group at the *ortho*-position in the B ring has high activity to donate its hydrogen atom to N- and O-centered radicals, whereas a *meta*-hydroxyl group has a high efficacy to reduce radicals. *o*-OH also possesses high activity to protect LH against autoxidation and to inhibit the oxidation of methyl linoleate induced by radicals. However, *o*-OH serves as a prooxidant in Cu^{2+}/GSH- and $^{\bullet}$OH-induced oxidations of DNA and as an antioxidant in AAPH-induced oxidation of DNA.

Supporting Information Available: Synthesis procedure of *o*-, *m*-, and *p*-HBMC and Figures S1−S3. This material is available free of charge via the Internet at http://pubs.acs.org.

LITERATURE CITED

(1) Mota, K. S. D.; Dias, G. E. N.; Pinto, M. E. F.; Luiz-Ferreira, A.; Souza-Brito, A. R. M.; Hiruma-Lima, C. A.; Barbosa-Filho, J. M.; Batista, L. M. Flavonoids with gastroprotective activity. *Molecules* **2009**, *14*, 979–1012.

(2) Matkowski, A. Plant in vitro culture for the production of antioxidants − a review. *Biotechnol. Adv.* **2008**, *26*, 548–560.

(3) Stevenson, D. E.; Hurst, R. D. Polyphenolic phytochemicals − just antioxidants or much more? *Cell. Mol. Life Sci.* **2007**, *64*, 2900–2916.

(4) Tian, L.; Pang, Y.; Dixon, R. A. Biosynthesis and genetic engineering of proanthocyanidins and (iso)flavonoids. *Phytochem. Rev.* **2008**, *7*, 445–465.

(5) Bovicelli, P.; D'Angelo, V.; Collalto, D.; Verzina, A.; D'Antona, N.; Lambusta, D. Efficient synthesis of polyoxygenated flavones from naturally occurring flavanones. *J. Pharm. Pharmacol.* **2007**, *59*, 1697–1701.
(6) Barve, V.; Ahmed, F.; Adsule, S.; Banerjee, S.; Kulkarni, S.; Katiyar, P.; Anson, C. E.; Powell, A. K.; Padhye, S.; Sarkar, F. H. Synthesis, molecular characterization, and biological activity of novel synthetic derivatives of chromen-4-one in human cancer cells. *J. Med. Chem.* **2006**, *49*, 3800–3808.
(7) Siddaiah, V.; Rao, C. V.; Venkateswarlu, S.; Krishnaraju, A. V.; Subbaraju, G. V. Synthesis, stereochemical assignments, and biological activities of homoisoflavonoids. *Bioorg. Med. Chem.* **2006**, *14*, 2545–2551.
(8) Severino, J. F.; Goodman, B. A.; Kay, C. W. M.; Stolze, K.; Tunega, D.; Reichenauer, T. G.; Pirker, K. F. Free radicals generated during oxidation of green tea polyphenols: electron paramagnetic resonance spectroscopy combined with density functional theory calculations. *Free Radical Biol. Med.* **2009**, *46*, 1076–1088.
(9) Lin, L.-G.; Xie, H.; Li, H.-L.; Tong, L.-J.; Tang, C.-P.; Ke, C.-Q.; Liu, Q.-F.; Lin, L.-P.; Geng, M.-Y.; Jiang, H.; Zhao, W.-M.; Ding, J.; Ye, Y. Naturally occurring homoisoflavonoids function as potent protein tyrosine kinase inhibitors by c-Src-based high-throughput screening. *J. Med. Chem.* **2008**, *51*, 4419–4429.
(10) Delazar, A.; Sabzevari, A.; Mojarrab, M.; Nazemiyeh, H.; Esnaashari, S.; Nahar, L.; Razavi, S. M.; Sarker, S. D. Free-radical-scavenging principles from *Phlomis caucasica*. *J. Nat. Med.* **2008**, *62*, 464–466.
(11) Rao, Y. K.; Geethangili, M.; Fang, S.-H.; Tzeng, Y.-M. Antioxidant and cytotoxic activities of naturally occurring phenolic and related compounds: a comparative study. *Food Chem. Toxicol.* **2007**, *45*, 1770–1776.
(12) Uppu, R. M.; Pryor, W. A. Synthesis of peroxynitrite in a two-phase system using isoamyl nitrite and hydrogen peroxide. *Anal. Biochem.* **1996**, *236*, 242–249.
(13) Maldonado, P. D.; Rivero-Cruz, I.; Mata, R.; Pedraza-Chaverri, J. Antioxidant activity of A-type proanthocyanidins from *Geranium niveum* (Geraniaceae). *J. Agric. Food Chem.* **2005**, *53*, 1996–2001.
(14) Re, R.; Pellegrini, N.; Proteggente, A.; Pannala, A.; Yang, M.; Rice-Evans, C. Antioxidant activity applying an improved ABTS radical cation decolorization assay. *Free Radical Biol. Med.* **1999**, *26*, 1231–1237.
(15) Yim, S.-K.; Yun, S.-J.; Yun, C.-H. A continuous spectrophotometric assay for NADPH-cytochrome P450 reductase activity using 1,1-diphenyl-2-picrylhydrazyl. *J. Biochem. Mol. Biol.* **2004**, *37*, 629–633.
(16) Bobrov, M. Y.; Lizhin, A. A.; Andrianova, E. L.; Gretskaya, N. M.; Frumkina, L. E.; Khaspekov, L. G.; Bezuglov, V. V. Antioxidant and neuroprotective properties of *N*-arachidonoyldopamine. *Neurosci. Lett.* **2008**, *431*, 6–11.
(17) Li, G.-X.; Liu, Z.-Q. Captopril and 6-mercaptopurine: whose SH possesses higher antioxidant ability? *Eur. J. Med. Chem.* **2009**, *44*, 4841–4847.
(18) Yu, J.; Wang, L.; Walzem, R. L.; Miller, E. G.; Pike, L. M.; Patil, B. S. Antioxidant activity of citrus limonoids, flavonoids, and coumarins. *J. Agric. Food Chem.* **2005**, *53*, 2009–2014.
(19) Li, G.-X.; Liu, Z.-Q. Unusual antioxidant behavior of α- and γ-terpinene in protecting methyl linoleate, DNA, and erythrocyte. *J. Agric. Food Chem.* **2009**, *57*, 3943–3948.
(20) Reed, C. J.; Douglas, K. T. Chemical cleavage of plasmid DNA by glutathione in the presence of Cu(II) ions. The Cu(II)-thiol system for DNA strand scission. *Biochem. J.* **1991**, *275*, 601–608.
(21) Zhu, B.-Z.; Kitrossky, N.; Chevion, M. Evidence for production of hydroxyl radicals by pentachlorophenol metabolites and hydrogen peroxide: a metal-independent organic Fenton reaction. *Biochem. Biophys. Res. Commun.* **2000**, *270*, 942–946.
(22) Zhao, F.; Liu, Z.-Q. The protective effect of hydroxyl-substituted Schiff bases on the radical-induced oxidation of DNA. *J. Phys. Org. Chem.* **2009**, *22*, 791–798.
(23) Zhao, B. Natural antioxidants protect neurons in Alzheimer's disease and Parkinson's disease. *Neurochem. Res.* **2009**, *34*, 630–638.
(24) Willmore, L. J.; Ueda, Y. Posttraumatic epilepsy: Hemorrhage, free radicals and the molecular regulation of glutamate. *Neurochem. Res.* **2009**, *34*, 688–697.
(25) Erel, O. A novel automated direct measurement method for total antioxidant capacity using a new generation, more stable ABTS radical cation. *Clin. Biochem.* **2004**, *37*, 277–285.
(26) Eklund, P. C.; Långvik, O. K.; Wärnå, J. P.; Salmi, T. O.; Willför, S. M.; Sjöholm, R. E. Chemical studies on antioxidant mechanisms and free radical scavenging properties of lignans. *Org. Biomol. Chem.* **2005**, *3*, 3336–3347.
(27) Fan, G.-J.; Liu, X.-D.; Qian, Y.-P.; Shang, Y.-J.; Li, X.-Z.; Dai, F.; Fang, J.-G.; Jin, X.-L.; Zhou, B. 4,4′-Dihydroxy-*trans*-stilbene, a resveratrol analogue, exhibited enhanced antioxidant activity and cytotoxicity. *Bioorg. Med. Chem.* **2009**, *17*, 2360–2365.
(28) Mena, S.; Ortega, A.; Estrela, J. M. Oxidative stress in environmental-induced carcinogenesis. *Mutat. Res.* **2009**, *674*, 36–44.
(29) Prütz, W. A. Interaction between glutathione and Cu(II) in the vicinity of nucleic acids. *Biochem. J.* **1994**, *302*, 373–382.
(30) Zheng, L.-F.; Dai, F.; Zhou, B.; Yang, L.; Liu, Z.-L. Prooxidant activity of hydroxycinnamic acids on DNA damage in the presence of Cu(II) ions: mechanism and structure−activity relationship. *Food Chem. Toxicol.* **2008**, *46*, 149–156.

Received for review November 20, 2009. Revised manuscript received February 21, 2010. Accepted February 21, 2010. We thank the National Natural Science Foundation, China, for financial support.